Tailoring Oxygen Content on $PrBaCo_2O_{5+\delta}$ Layered Cobaltites

C. Frontera,*,† A. Caneiro,‡ A. E. Carrillo,† J. Oró-Solé,† and J. L. García-Muñoz†

Institut de Ciéncia de Materials de Barcelona, CSIC, Campus Universitari de Bellaterra, 08193 Bellaterra, Spain, and Centro Atómico Bariloche, 8400-San Carlos de Bariloche, Argentina

Received May 31, 2005. Revised Manuscript Received August 21, 2005

The $LnBaCo_2O_{5+\delta}$ cobaltites with ordered A-site cations exhibit a very rich phase diagram as a function of the oxygen content, which determines the doping of CoO_2 planes. By means of thermogravimetry analysis (TGA), we study the appropriate way to tailor oxygen contents in $PrBaCo_2O_{5+\delta}$ compounds. Starting from an air-synthesized sample, we study the evolution of δ during different heat treatments with "in situ" TGA measurements. We find that δ can be tailored from $\delta \simeq 0.2$ to $\delta \simeq 0.9$. Thermogravimetry measurements also show that oxygen ions can flow through (0 0 1) PrO_δ planes at relatively low temperatures (200 °C, this temperature increases in compounds with smaller rare earths). By means of neutron powder diffraction at room temperature, we determine the structural details and study the eventual order of oxygen vacancies for different values of δ.

1. Introduction

Exploration of layered cobaltites in a search for unusual behavior derived from strong electron correlations and coupling between spin, charge, orbital, and lattice degrees of freedom is revealing a rich variety of properties that brings about a renewed interest for these challenging materials. So, different families of Co oxides manifest fascinating properties. They are related, for instance, to orbital physics phenomena, conductivity and magnetic transitions derived from changes in the spin state of Co, charge ordering, giant MR, nanoscopic phase separation, large thermoelectric power, and so forth. Even the occurrence of unconventional superconductivity has been recently confirmed in a layered cobalt system.[1] From these findings, it is now apparent that cobalt oxides belong to the group of strong correlated transition metal oxides presenting a most rich behavior and challenging properties.

Layered cobaltites ($LnBaCo_2O_{5+\delta}$, Ln = rare earth; $0 \leq \delta \leq 1$) have been the subject of growing research activity during recent years. Although some previous reports on these materials are slightly older (e.g., refs 2 and 3), from the study of "$Gd_{0.5}Ba_{0.5}CoO_3$" by Troyanchuck et al.[4] reporting a metal insulator and two magnetic transitions, a vivid interest in these compounds has surged.[5−19] Maignan et al.[5] established that these cobaltites present two main structural features. The first one is that lanthanide and Ba ions do not form a solid solution at the A position of the perovskite structure but order in alternating (0 0 1) layers. As happens in many doped cobaltites, these compounds have a strong tendency to present oxygen vacancies ($\delta < 1$). The second structural feature is that these vacancies locate at the Ln layers with a great tendency to form ordered patterns. This results in a coexistence of Co ions in octahedral (CoO_6) and pyramidal (CoO_5) environments in an ordered manner. Maignan et al.[5] also showed that δ can be easily varied by means of heat treatments under appropriate atmospheres and evidenced that the magnetic and transport properties are highly dependent on the oxygen content. In fact, δ controls the nominal valence of Co ions that varies from 3.5+ (50% of Co^{3+} and 50% of Co^{4+}) for $\delta = 1$ to 2.5+ (50% of Co^{3+} and 50% of Co^{2+}) for $\delta = 0$, passing through 100% of Co^{3+} for $\delta = 0.5$. In this scenario, different interesting properties have been reported for different oxygen contents. For $\delta = 0$, charge

* Author to whom correspondence should be addressed. Phone: +34 935 801 852 ext. 309. Fax: +34 935 805 729. E-mail: frontera@icmab.es.
† Institut de Ciéncia de Materials de Barcelona, CSIC.
‡ Centro Atómico Bariloche.

(1) Takada, K.; Sakurai, H.; Takayama-Muromachi, E.; Izumi, F.; Dilanian, R. A.; Sasaki, T. *Nature* **2003**, *422*, 53.
(2) Zhou, W.; Lin, C. T.; Liang, W. Y. *Adv. Mater.* **1993**, *5*, 735.
(3) Zhou, W. *Chem. Mater.* **1994**, *6*, 441.
(4) Troyanchuk, I. O.; Kasper, N. V.; Khalyavin, D. D.; Szymczak, H.; Szymczak, R.; Baran, M. *Phys. Rev. Lett.* **1998**, *80*, 3380.
(5) Maignan, A.; Martin, C.; Pelloquin, D.; Nguyen, N.; Raveau, B. *J. Solid State Chem.* **1999**, *142*, 247.
(6) Akahoshi, D.; Ueda. Y. *J. Phys. Soc. Jpn.* **1999**, *68*, 736.
(7) Vogt, T.; Woodward, P. M.; Karen, P.; Hunter, B. A.: Henning, P.; Moodenbaugh, A. R. *Phys. Rev. Lett.* **2000**, *84*, 2969.
(8) Suard, E.; Fauth, F.; Caignaert, V.; Mirebeau, I.; Baldinozzi, G. *Phys. Rev. B* **2000**, *61*, R11871.
(9) Moritomo, Y.; Akimoto, T.; Takeo, M.; Machida, A.; Nishibori, E.; Takata, M.; Sakata, M.; Ohoyama, K.; Nakamura, A. *Phys. Rev. B* **2000**, *61*, R13325.
(10) Respaud, M.; Frontera, C.; García-Muñoz, J. L.; Aranda, M. A. G.; Raquet, B.; Broto, J. M. *Phys. Rev. B* **2001**, *64*, 214401.
(11) Akahoshi, D.; Ueda. Y. *J. Solid State Chem.* **2001**, *156*, 355.
(12) Frontera, C.; García-Muñoz, J. L.; Llobet, A.; Aranda, M. A. G. *Phys. Rev. B* **2002**, *65*, 180405R.
(13) Fauth, F.; Suard, E.; Caignaert, V.; Mirebeau, I. *Phys. Rev. B* **2002**, *66*, 184421.
(14) Burley, J. C.; Mitchell, J. F.; Short, S.; Miller, D.; Tang. Y. *J. Solid State Chem.* **2003**, *170*, 339.
(15) Taskin, A. A.; Lavrov, A. N.; Ando,Y. *Proceedings of the 22nd International Conference on Thermoelectrics*, Hérault, France, August 2003, p 196.
(16) Taskin, A. A.; Lavrov, A. N.; Ando, Y. *Phys. Rev. Lett.* **2003**, *90*, 227201.
(17) Khalyavin, D. D.; Barilo, S. N.; Shiryaev, S. V.; Bychkov, G. L.; Troyanchuck, I. O.; Furrer, A.; Allenspach, A.; Szymczak, H.; Szymczak, R. *Phys. Rev. B* **2003**, *67*, 214421.
(18) Soda, M.; Yasui, Y.; Fujita, T.; Miyashita, T.; Sato, M.; Kakurai, K. *J. Phys. Soc. Jpn.* **2003**, *72*, 1729 (also, cond-mat/0301618).
(19) Maignan, A.; Caignaert. V.; Raveau, B.: Khomskii, D.; Sawatzky, G. *Phys. Rev. Lett.* **2004**, *93*, 026401.

10.1021/cm051148q CCC: $30.25
Published on Web 10/07/2005

ordering between Co^{3+} and Co^{2+} has been reported.[7,8] For $\delta = 0.5$, a metal insulator transition is shown independently of the rare earth.[5] This transition was initially attributed to orbital order phenomena; later, it was ascribed to a spin-state transition of Co in an octahedral place,[12,20] although this picture is not free from controversy.[13,21] More recently, with the aid of thermopower measurements, a "spin blockade" mechanism was proposed for this metal−insulator transition.[19]

Different heat treatments under different atmospheres have been used to vary the oxygen content in $NdBaCo_2O_{5+\delta}$ (within the range $0 \leq \delta \leq 0.69$)[14] and in single crystals of $GdBaCo_2O_{5+\delta}$ (within the range $0 \leq \delta \leq 0.77$).[22] In this paper, we present two sets of "in situ" thermogravimetry analysis (TGA) studies of $PrBaCo_2O_{5+\delta}$. The first is done under different atmospheres and varying the temperature. The second is done at fixed temperature and varying the oxygen partial pressure. The first set of measurements evidences that oxygen can move easily through PrO_δ planes at temperatures above $T \simeq 200$ °C. This has been confirmed by means of neutron powder diffraction (NPD) in the range from room temperature (RT) to 350 °C. With the aid of the second set of measurements, it becomes possible to plan adequate heat treatments to get the desired δ for this rare earth. To illustrate this, we have prepared two samples with rational oxygen content $\delta \simeq 1/2$ and $\delta \simeq 3/4$. In addition, we have tried to open as wide as possible the δ range by preparing a sample with a quite low oxygen content, $\delta \simeq 0.17$, and a sample with $\delta \simeq 0.87$ by means of moderately high oxygen pressure. All samples have been studied by means of NPD at RT to gain insight into the order of vacancies. Obviously, the method can be used for other rare earth elements, and this study contributes to the establishment of the protocols for the synthesis of these interesting oxides with the desired δ values.

2. Experimental Section

The initial polycrystalline sample has been synthesized by a solid-state reaction in air. High-purity oxides (Pr_6O_{11} and Co_3O_4) and carbonates ($BaCO_3$) were mixed at stoichiometric ratios. After two decarbonating treatments at 900 °C with intermediate grinding, the resulting product was pressed into a pellet at 10 Tm, finally fired at 1100 °C over 12h in air, and cooled to RT at −100 °C/hour. The quality of the product obtained was tested by X-ray diffraction. This revealed that the sample is in a single phase and that no impurities can be detected with this technique. The oxygen content of this "as-synthesized" sample was found to be $\delta = 0.763(3)$.

Further, small portions of the "as-synthesized" compound were measured by TGA up to 800 °C in pure O_2, air, and pure Ar atmospheres using a Perkin-Elmer (model TGA-7) thermogravimetric analyzer.

The equilibrium oxygen partial pressure (P_{O_2}) as a function of T and δ in $PrBaCo_2O_{5+\delta}$ was obtained by thermogravimetry[23] within the ranges 250 °C < T < 900 °C and 10^{-5} atm < P_{O_2} < 1 atm.

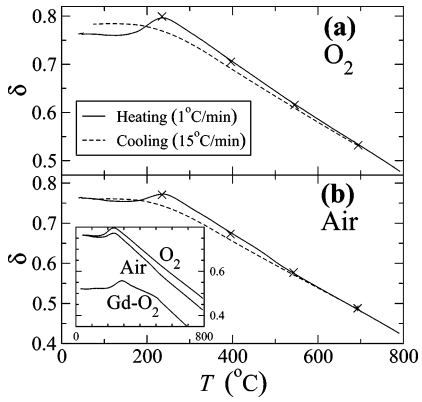

Figure 1. TGA measurement of δ as a function of temperature for slow heating (1 °C/min, solid lines) and rapid cooling (15°C/min, dashed lines) processes in (a) O_2 and (b) air atmospheres. The crosses mark the value of δ obtained at the corresponding temperature after a long annealing. The inset shows a comparison of heating curves of $PrBaCo_2O_{5+\delta}$ under O_2 and air. The inset also shows the evolution of δ under O_2 at the same conditions obtained for $GdBaCo_2O_{5+\delta}$.

This is achieved by varying P_{O_2} at constant temperature and measuring the weight variations of the sample.

With the aid of these measurements, samples with controlled oxygen content were prepared by annealing the as-made samples at the appropriate temperatures under the appropriate oxygen partial pressure over 24 h and quenching them to liquid-nitrogen temperatures. The absolute oxygen content of the precursors and quenched samples was checked by reduction in a dry 10% H_2/Ar mixture at 1000 °C assuming Co, Pr_2O_3, and BaO as final products. The so-determined values of δ were close (within ±0.004) to those corresponding to the equilibrium P_{O_2} measurements.

NPD patterns were collected for all prepared samples using a D2B diffractometer ($\lambda = 1.594$ Å, at 10′ collimation mode; ILL, Grenoble, France) at RT. In addition, for one of the prepared compounds, we have collected NPD patterns using a high-flux D1B diffractometer ($\lambda = 2.52$ Å; ILL, Grenoble, France) in the temperature range from RT to 360 °C.

Magnetization measurements were done using a SQUID (Quantum Design) under $\mu_0 H = 0.1$ T of applied field after cooling under the same magnetic field.

3. Results and Discussion

3.1. Heat Treatments under Different Atmospheres and Oxygen Partial Pressures. Figure 1 shows the evolution of δ under an O_2 atmosphere (Figure 1a) and under air (Figure 1b) when the sample is slowly heated at a rate of 1 °C/min (a comparison of both curves is drawn in the inset of Figure 1b). After the final temperature (800 °C) was reached, the samples were cooled to RT at a rate of 15 °C/min. To compare the values of δ obtained during the slow heating with those corresponding to the equilibrium, we have performed a second set of measurements at constant temperature over about 3 h (achieved after a quick heating). We have observed that, after the initial 40 min, no more variation of δ is detected. The obtained values are also depicted in Figure 1 as crosses. The coincidence between both sets of values is remarkable. This indicates that the $\delta(T)$ dependence obtained by slow heating is very near the equilibrium one.

Some features evidenced in Figure 1 must be discussed. It can be seen that the oxygen lost during the heating process is recovered during the cooling process. Thus, the final value of δ after the heating−cooling cycle under air is almost

(20) Kusuya, H.; Machida, A.; Moritomo, Y.; Kato. K.; Nishibori, E.; Takata, M.; Sakata, M.; Nakamura, A. *J. Phys. Soc. Jpn.* **2001**, *70*, 3577.
(21) Wu, H. *Phys. Rev. B* **2001**, *64*, 092413.
(22) Taskin, A. A.; Lavrov, A. N.; Ando, Y. *Phys. Rev. B* **2005**, *71*, 134414.
(23) Caneiro, A.; Bavdaz, P.; Fouletier. J.; Abriata, J. P. *Rev. Sci. Instrum.* **1982**, *53*, 1072.

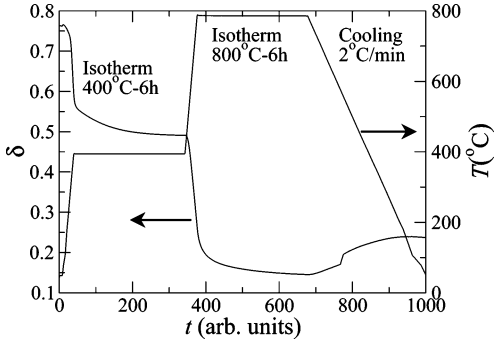

Figure 2. TGA measurement of δ during the plotted heat treatment under an Ar atmosphere. We note the enhancement of δ during the final cooling.

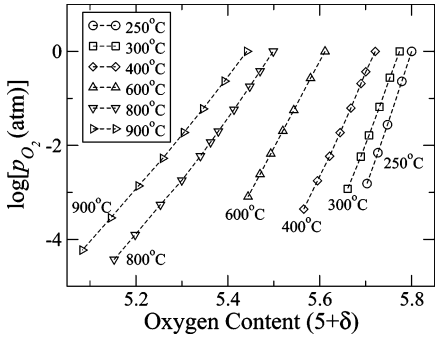

Figure 3. Isothermal changes of the oxygen content as a function of oxygen partial pressure for different temperatures.

identical to the initial value, and under O_2, it is slightly greater. Another important feature to discuss is the mobility of oxygen. It can be appreciated that, when heating, a certain oxygen gain is achieved from about 175−200 °C and that a maximum is achieved at about 240 °C. To make possible this oxygen gain, two different subprocesses must take place. The first one is the absorption of oxygen at the surface of the material (governed by the chemical surface reactivity), and the second is diffusion toward the bulk of the absorbed oxygen (governed by the diffusion coefficient). The enlargement of δ depicted in Figure 1 evidences that the oxygen can be absorbed and can diffuse in PrO_δ planes at relatively low temperatures. It is also evidenced that, in order to get a large value of δ, one must anneal under O_2 and that it makes no sense to heat above 240 °C. These temperatures are smaller than (but not far from) those reported for $YBaCo_2O_{5+\delta}$ when the oxygen mobility has been detected at about 230 °C.[6] To gain insight into the possible dependence on Ln of the temperature when oxygen starts to diffuse within LnO_δ planes, we have done TGA measurements under an oxygen atmosphere for $GdBaCo_2O_{5+\delta}$ using the same heating velocity (1 °C/min). The result obtained is shown in the inset of Figure lb. From this inset, it can be appreciated that the oxygen starts to flow through $GdBaCo_2O_{5+\delta}$ at a temperature slightly larger (the difference is about 25 °C) than that for $PrBaCo_2O_{5+\delta}$.

We have also measured the evolution of the oxygen content under an Ar atmosphere by the same procedure. However, we have failed in obtaining curves near equilibrium like those presented in Figure 1. The reason must be that the time needed to equilibrate the samples is much longer than that in air or O_2 atmospheres. This is illustrated in Figure 2. This figure shows the time evolution of δ, together with the temperature profile, under a pure Ar atmosphere. The study has six parts: (i) annealing for 10 min at 40 °C, (ii) a rapid heating (10 °C/min) to 400 °C, (iii) annealing at 400 °C for 6 h, (iv) rapid heating (10 °C/min) to 800 °C, (v) annealing at 800 °C for 6 h, and (vi) slow cooling (−2 °C/min) to RT. At both 400 and 800 °C, the time needed for equilibration is quite long. From this figure, it can be appreciated that the oxygen content can be reduced to about $\delta = 0.15$ at $T = 800$ °C. Another interesting point in Figure 2 is that the oxygen content increases again when the sample is slowly cooled to RT. It must be pointed out that this slow cooling is necessary to get the order of oxygen vacancies within the PrO_δ planes. The origin of this oxygen (in a pure Ar atmosphere) can come from two sources. It can come from the small impurities in the Ar gas (nominally 50 ppm molar), or more likely, it can come from a lack of hermeticity of the whole setup that would allow a certain fraction of oxygen to reach the sample.

A second set of measurements has been done using heat treatments under different oxygen partial pressures. The results obtained are summarized in Figure 3. This figure shows the isotherms of equilibrium P_{O_2} as a function of the oxygen content $5 + \delta$. All isotherms were reproducible upon oxidation (reduction) and subsequent reduction (oxidation). Therefore, they must be considered stable equilibrium states of the $PrBaCo_2O_{5+\delta}$ material. The equilibrium times were a few minutes for the high T and P_{O_2} ranges and some hours, and eventually up to 2 days, for low T and P_{O_2} values.

3.2. Heat Treatments and Sample Preparation. The preceding results have been used to prepare samples with four different oxygen contents. For the first three samples, the target oxygen levels were $\delta = 0.17$, 0.5, and 0.75. As explained in the Introduction, the second and third values correspond to the fractional values $^1/_2$ and $^3/_4$. The first one is very near the lowest value available. From Figure 3, the lowest value found is $\delta \simeq 0.08$, but the dynamics at very low P_{O_2} are very slow, and the preparation of a large amount of sample (∼3−4 g) with this δ value would require very long times. For these three samples, we chose appropriate heat treatments, and afterward, we quenched the samples from each temperature and pressure to liquid nitrogen temperatures.

According to Figure 3, $\delta \simeq 0.17$ is found on the $T = 900$ °C isotherm at an oxygen partial pressure $P_{O_2} = 5.07 \times 10^{-4}$ atm. We first annealed the sample under these conditions for 36 h. The oxygen content found after this first treatment was $\delta \simeq 0.25$. We performed a second treatment under the same conditions for 48 h more and determined a final oxygen content $\delta = 0.176(6)$. The second sample was prepared at 600 °C and $P_{O_2} = 5.55 \times 10^{-3}$ atm, where the value $\delta \simeq 0.5$ is found in Figure 3, over 36 h, and the final oxygen content determined was $\delta = 0.519(7)$. The last one was prepared at 250 °C and $P_{O_2} = 3.28 \times 10^{-2}$ atm over 36 h, and the final oxygen content determined was $\delta = 0.74(1)$. In addition, we have unsuccessfully tried to enhance the order of oxygen vacancies by taking a part of the $\delta = 0.519(7)$ sample and annealing it for 9 h at 180 °C in an ultrahigh vacuum. The oxygen content of this annealed sample was determined to be $\delta = 0.50(1)$.

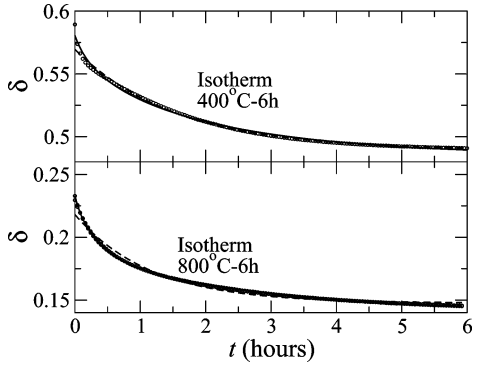

Figure 4. Fitting to the isothermal decay of δ, under an Ar atmosphere, following expressions 1 (solid lines) and 2 (dashed lines). It can be appreciated that data corresponding to $T = 800$ °C are well-fitted by expression 1, but data corresponding to $T = 400$ °C cannot be well-fitted by either of these two expressions.

The fourth sample was prepared by means of high oxygen pressure ($P_{O_2} = 180$ atm). We first heated the sample at 1 °C/min up to 216 °C. After 48 h, we cooled it down to 190 °C at the same rate and kept it there for 10 h. We finally cooled the sample down to RT at 1 °C/min. The oxygen content was determined to be $\delta = 0.87(1)$.

3.3. Kinetics of Oxygen Changes. Relaxation toward equilibrium has been used to obtain information about the diffusion coefficient (D) and chemical surface reaction coefficient (K) in single crystals with a parallelepiped shape where an analytical solution of the diffusion equation exists.[24−26] In powder samples, the situation is different as the shape and size of the grains are not known precisely. Despite this difficulty, previous works have studied the kinetics of oxygen change in powder samples by assuming that grains are spheres of average radius R.[27] With this hypothesis, when the oxygen content is limited by the diffusion coefficient D, the variation of δ must follow[27]

$$\frac{\delta - \delta_e}{\delta_0 - \delta_e} = \frac{6}{\pi^2}\sum_{n=1}^{N}\frac{1}{n^2}\exp\left(-n^2\frac{D\pi^2}{R^2}t\right) \qquad (1)$$

where δ_e and δ_0 are the equilibrium and initial values of δ, respectively. The decay toward equilibrium in this expression is given by the characteristic time $R^2/D\pi^2$. We have tried to fit this expression to the data in Figure 2. The results are shown in Figure 4 as solid lines. It can be realized that eq 1 fits well the data obtained at 800 °C but fails in reproducing the data at 400 °C, indicating that at lower temperatures, the surface reactivity is also relevant.

Taskin et al.[22] have also studied the kinetics on powder samples. These authors found that the relaxation toward equilibrium of $GdBaCo_2O_{5+\delta}$ can be well-described using a single exponential and that this indicates that the process is mainly governed by oxygen interchange at the surface. We have tried to describe the data in Figure 4 by means of a single exponential:

$$\frac{\delta - \delta_e}{\delta_0 - \delta_e} = \exp\left(\frac{-t}{\tau}\right) \qquad (2)$$

The best fits to this expression are shown in Figure 4 as dashed lines. It is worth mentioning that fits done using eq 1 have the same number of free (refinable) parameters as those using eq 2. It can be appreciated that the experimental data are not reproduced well by this expression. This means that bulk diffusion is more relevant than surface exchange in $PrBaCo_2O_{5+\delta}$, at least at high temperatures, and it opens the question of how K and D depend on the size of the rare earth element in the $LnBaCo_2O_{5+\delta}$ family.

It is also worth noting that the decay time τ is less than 2.5 h at both 400 and 800 °C under an Ar atmosphere. As we have commented in subsection 3.1, this time is shorter under an oxygen atmosphere.

3.4. Characterization of the Sintered Samples. We have collected high-resolution NPD patterns at RT for the four samples prepared. These patterns show that all samples are single-phased and well-crystallized. This warrants that both the oxygen content and the order of oxygen vacancies achieved by means of the heat treatments used are homogeneous. NPD patterns corresponding to $\delta \simeq 0.18$, 0.75, and 0.87 can be indexed with tetragonal lattices, but for $\delta \simeq 0.50$, an orthorhombic lattice is needed. Refinements have been done using the *P*4/*mmm* space group (No. 123) when the lattice is tetragonal and using the *Pmmm* space group (No. 47) when it is orthorhombic. The structures found are detailed in Table 1 and sketched in Figure 5. NDP data confirm the ordering of oxygen vacancies in alternating rows found for other $LnBaCo_2O_{5+\delta}$ compounds with $\delta \simeq 0.50$,[5,6,9,12,14] although Rietveld refinements point toward an imperfect order. In fact, a perfectly ordered sample[5,9] would present 100% of the oxygen occupancy at Wyckoff position 1*g* and 0% at the 1*c* position (space group *Pmmm*), but we have gotten occupancies of 91(3)% and 12(3)%, respectively, as printed in Table 1. We have also found evidences of oxygen ordering in the $\delta \approx 0.75$ compound.[28] This order consists of a partial filling of Wyckoff positions 1*b* [35(3)%] and 1*d* [63(3)%] of the *P*4/*mmm* space group. The other Wyckoff position within the $PrO_{0.75}$ planes, position 2*e*, is fully occupied. No vacancy ordering has be detected in the $\delta \simeq 0.87$ and $\delta \simeq 0.18$ samples, thus, leading to the $a_p \times a_p \times 2a_p$ cell reported in Table 1. It is worth mentioning that neutron data corresponding to $\delta \simeq 0.18$ show long-range antiferromagnetic ordering at RT. Magnetic peaks can be well-fitted by using a G-type magnetic structure [with an ordered moment of 2.3(2) μB/Co] as reported for $\delta = 0$ compounds.[7,8] Consistently, the reported temperatures where magnetic order appears in the $\delta = 0$ compounds are above RT.

NPD data allow the refinement of the oxygen content of the samples. Refined oxygen contents coincide with those obtained by TGA (reducing the samples in dry H_2 at 1000 °C) except for the case $\delta \simeq 0.18$, where the value obtained by NPD is $\delta = 0.24(4)$. It is also worth mentioning that we

(24) Yasuda, I.; Hishinuma, M. *J. Solid State Chem.* **1996**, *123*, 382.
(25) Lane, J. A.; Kilner, J. A. *Solid State Ionics* **2000**, *136−137*, 997.
(26) Taskin, A. A.; Lavrov, A. N.; Ando, Y. *Appl. Phys. Lett.* **2005**, *86*, 091910.
(27) Prado, F.; Caneiro, A.; Serquis, A.; Briatico, J. *Solid State Commun.* **1995**, *94*, 75.
(28) Frontera, C.; García-Muñoz, J. L.; Carrillo, A. E.; Ritter, C.; Martin y Marero, D.; Caneiro, A. *Phys. Rev. B* **2004**, *70*, 184428.

Table 1. Structural Details of the Prepared Samples Obtained by Means of High Resolution NPD[a]

δ	0.176(6)	0.50(1)	0.74(1)	0.87(1)
SG	*P4/mmm*	*Pmmm*	*P4/mmm*	*P 4/mmm*
a (Å)	3.9373(4)	3.9049(4)	7.8218(9)	3.8947(4)
b (Å)		7.8733(9)		
c (Å)	7.6053(9)	7.6084(9)	7.6353(8)	7.6353(9)
V/Z (Å^3)	58.9(1)	58.5(1)	58.2(1)	57.9(1)
Ba	1*b* ($^1/_2$, $^1/_2$, 0)	2*o* ($^1/_2$, *y*, 0) *y* = 0.2483(5)	4*j* (*x*, *x*, 0) *x* = 0.2500(7)	1*b* ($^1/_2$, $^1/_2$, 0)
Pr	1*d* ($^1/_2$, $^1/_2$, $^1/_2$)	2*p* ($^1/_2$, *y*, $^1/_2$) *y* = 0.2712(7)	4*k* (*x*, *x*, $^1/_2$) *x* = 0.2575(7)	1*d* ($^1/_2$, $^1/_2$, $^1/_2$)
Co1	2*g* (0, 0, *z*) *z* = 0.2525(7)	2*q* (0, 0, *z*) *z* = 0.253(1)	2*g* (0, 0, *z*) *z* = 0.249(2)	2*g* (0, 0, *z*) *z* = 0.2485(7)
Co2		2*r* (0, $^1/_2$, *z*) *z* = 0.250(1)	2*h* ($^1/_2$, $^1/_2$, *z*) *z* = 0.248(2)	
Co3			4*i* ($^1/_2$, 0, *z*) *z* = 0.251(1)	
O1a	1*a* (0, 0, 0)	1*a* (0, 0, 0)	1*a* (0, 0, 0)	1*a* (0, 0, 0)
O1b		1*e* (0, 1, 0)	1*c* ($^1/_2$, $^1/_2$, 0)	
O1c			2*f* (0, $^1/_2$, 0)	
O2a	1*b* (0, 0, $^1/_2$) Occ. = 0.24(4)	1*c* (0, 0, $^1/_2$) Occ. = 0.12(3)	1*b* (0, 0, $^1/_2$) Occ. = 0.35(3)	1*b* (0, 0, $^1/_2$) Occ. = 0.86(3)
O2b		1*g* (0, $^1/_2$, $^1/_2$) Occ. = 0.91(3)	1*d* ($^1/_2$, $^1/_2$, $^1/_2$) Occ. = 0.63(3)	
O2c			2*e* (0, $^1/_2$, $^1/_2$)	
O3a	4*i* (0, 1/2, *z*) *z* = 0.2932(6)	2*s* ($^1/_2$, 0, *z*) *z* = 0.306(1)	8*s* (*x*, 0, *z*) *x* = 0.244(1) *z* = 0.2875(5)	4*i* (0, $^1/_2$, *z*) *z* = 0.2744(7)
O3b		2*t* ($^1/_2$, $^1/_2$, *z*) *z* = 0.266(1)	8*t* (*x*, $^1/_2$, *z*) *x* = 0.250(1) *z* = 0.2702(6)	
O3c		4*u* (0, *y*, *z*) *y* = 0.2405(8) *z* = 0.2850(8)		
$\langle d_{Co1-O} \rangle$	1.974(2)	1.944(4)	1.923(7)	1.942(2)
$\langle d_{Co2-O} \rangle$		1.974(2)	1.949(7)	
$\langle d_{Co3-O} \rangle$			1.963(5)	

[a] The position occupied by each atom is accompanied with the symbol of the corresponding Wyckoff position. Oxygen atoms labeled as O1α (with α = a, b, or c) correspond to oxygen in BaO planes, those labeled as O2α correspond to oxygen in PrO_δ planes (thus, the occupancy factor found is given), and those labeled as O3α correspond to oxygen in CoO_2 planes. Mean Co−O bond distances, defined as $\langle d_{Coi-O} \rangle = \sum_{j=1}^{6} w_j d_{Coi-O} / \sum_{j=1}^{6} w_j$ (where the weight w_j is the occupancy of oxygen O_j), are also given. Occ. = occupancy factor.

have also checked the order between Pr and Ba. Results of the test indicate that these two cations are well-ordered and no evidence of significant mixing between them has been found. It must be recalled that the Fermi lengths of Ba and Pr are quite similar [5.07(3) fm and 4.58(5) fm, respectively], so the contrast of these two atoms by NPD is about 10%. Although this contrast must be enough to elucidate the degree of order between them, we have reinforced these evidences by refining the occupancies of oxygen ions at the BaO planes. In accordance, we have determined that no oxygen vacancies are present at those planes. Final refinements (reported in Table 1) have been done assuming a perfect ordering between Pr and Ba.

Figure 6 shows the evolution of the unit cell volume per formula unit. The cell volume expands when lowering the oxygen content δ. This could seem contradictory, but it must be ascribed to changes in Co valence due to changes in δ. High δ values imply a coexistence of Co^{4+} and Co^{3+}, while values below $\delta = 0.5$ imply the coexistence of Co^{3+} and Co^{2+}. From ionic radii reported by Shannon[29] ($r^{VI}_{Co^{4+}} = 0.53$ Å, $r^{VI}_{Co^{3+}} = 0.61$ Å, and $r^{VI}_{Co^{2+}} = 0.745$ Å), a growth of Co size accompanies the reduction of δ. Accordingly, we found an enlargement of the mean Co−O bond distances as δ decreases (see Table 1). This enlargement of the Co cation counterbalances the effect of oxygen loss and enlarges the unit cell volume. Figure 7 shows the evolution of magnetization for $\delta \simeq 0.18$, 0.50, and 0.75. The smallest magnetic moment corresponds to $\delta \simeq 0.18$ compounds that, as stressed above, present AFM peaks in the NPD pattern corresponding to RT. The $\delta \simeq 0.50$ compound presents first, on cooling from RT, an enhancement of the magnetic moment, followed by a drop of this moment. This behavior resembles that reported for other compounds with the same oxygen content.[5,10,11] The $\delta \simeq 0.75$ compound presents a stronger ferromagnetic moment as corresponds to the canted antiferromagnetic structure reported at low *T*.[28] The results in Figure 7 reinforce the strong dependence of the magnetic properties of these compounds on the oxidation state of the Co ions as well as on their environment.

To gain insight into the temperature range when the oxygen mobility starts, we have collected NPD data in the range from RT to 360 °C on the sample with $\delta \simeq 0.87$ (the initial value). Figure 8 shows an intensity map from NPD data obtained in the region corresponding to (1 0 0) and (0 0 2) reflections. The evolution of the position of the maxima in Figure 8 evidences a sudden growth of a lattice parameter at about 200 °C. According to the results in Figures 1 and 6, this sudden enlargement must be ascribed to the loss of oxygen from this temperature.

(29) Shannon, R. D. *Acta Crystallogr., Sect. A* **1976**, *A32*, 751.

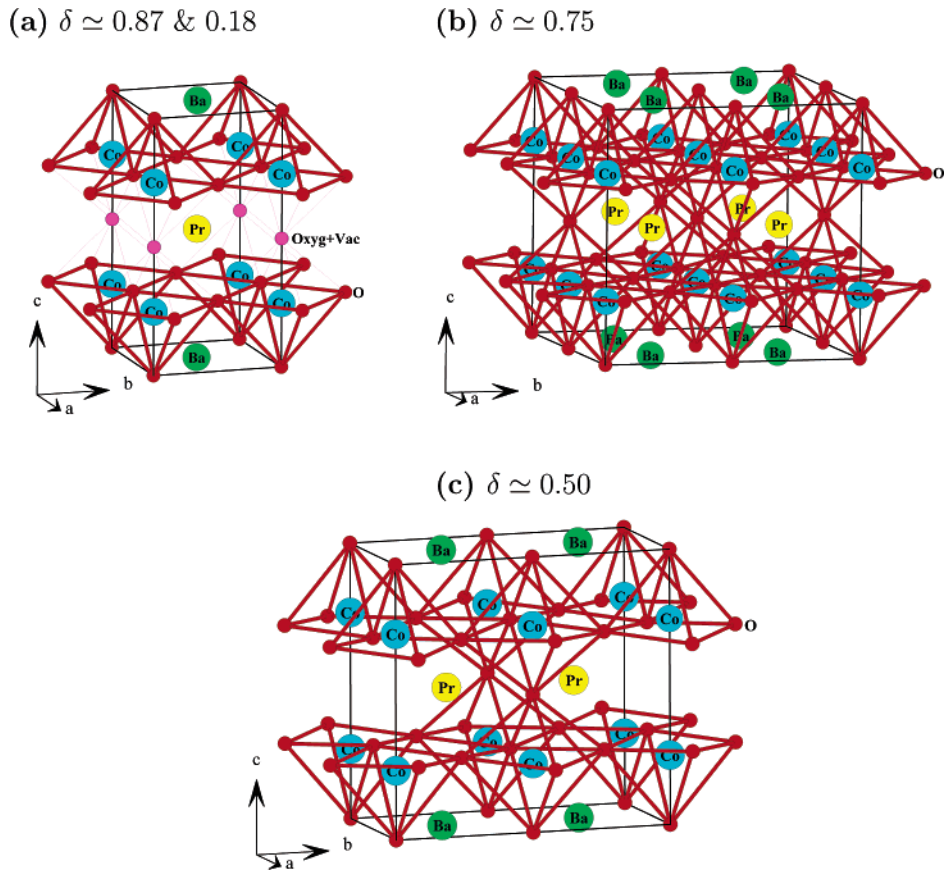

Figure 5. Sketched structure found by NPD for the different samples prepared. (a) The $\delta \simeq 0.87$ and $\delta \simeq 0.18$ cases where the cell found is tetragonal (*P4*/*mmm* SG) with $a \sim a_p$ and $c \sim 2 \times a_p$ and vacancies and oxygen ions are randomly mixed in the 1*b* Wyckoff position. Accordingly, Co ions are coordinated in pyramids and octahedra in a random way. (b) The idealized structure for the $\delta \simeq 0.75$ case, with tetragonal (*P4*/*mmm* SG) symmetry and $a \sim c \sim 2 \times a_p$; in this case, vacancies are placed at the l*b* Wyckoff position. (c) The $\delta \simeq 0.50$ case with vacancies along (1 0 0) lines; in this case, the cell is orthorhombic. For $\delta \simeq 0.75$ and 0.50, CoO_6 octahedra and CoO_5 pyramids coexist in an ordered way.

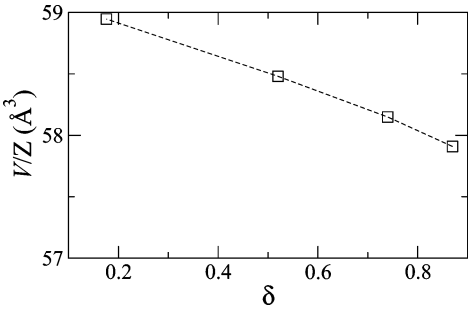

Figure 6. Dependence on δ of the cell volume per formula unit as found from neutron powder diffraction data on prepared samples.

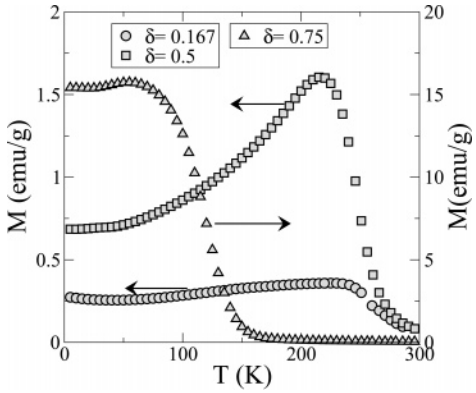

Figure 7. Magnetization found for the $\delta \simeq 0.18$, 0.50 (left axis), and 0.75 (right axis) compounds with an applied field of 1000 Oe.

4. Summary and Conclusions

A great deal of effort is being made to determine the rich and complex phase diagrams of $LnBaCo_2O_{5+\delta}$. Although a key parameter in the phase diagrams is the oxygen content, detailed investigations focused on the equilibrium oxygen contents (as a function of temperature and oxygen partial pressure), the specific behavior of oxygen kinetics and oxygen diffusion, and the tendency of oxygen vacancies to form ordered patterns in the LnO_δ planes are very scarce or clearly lacking. With the objective of giving a response to some of these questions, we have performed detailed research on the $PrBaCo_2O_{5+\delta}$ system on the basis of thermogravimetry and neutron diffraction measurements. Different "in situ" thermogravimetry analyses were done. The dependence of the oxygen vacancy content upon temperature was determined for different annealing atmospheres: air, O_2, and pure Ar. For that, two procedures were followed: (i) long-time annealing and (ii) slow, continuous heating.

Long-time annealing was done at selected temperatures in the interval RT to 800 °C. We determined that, in air or O_2 atmospheres, annealing times of about 2 h are enough to bring the system to equilibrium in the case of powder samples (~0.1 g polycrystalline samples). Longer annealing times did not produce modifications of the oxygen stoichiometry. Hence, the kinetics of the oxygen exchange are rather fast in the system. Moreover, continuous heating treatments using slow heating rates (1 °C/min) were used to establish the continuous $\delta - T$ dependence in air or O_2 atmospheres. With

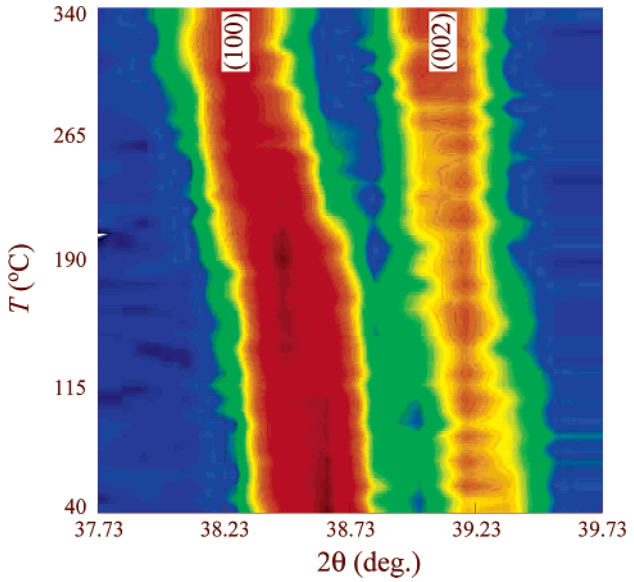

Figure 8. Intensity map (from NPD data) showing (1 0 0) and (0 0 2) diffraction peaks of "$PrBaCo_2O_{5.87}$" as a function of temperature. The shift toward low 2θ evidences a sudden enlargement of a cell parameter due to oxygen losses.

this heating rate, the system is very near the equilibrium and no differences were found with respect to the long-time annealing measurements. A maximum in the oxygen content is found at $T \simeq 240$ °C. According to the observation of fast oxygen exchange kinetics, only slight differences in δ-(T) curves were observed in the interval 240−500 °C when cooling $PrBaCo_2O_{5+\delta}$ samples with cooling rates 15 times faster compared to those of the slow heating. A remarkable finding is the observation that oxygen intercalation is already observed at $T \simeq 200$ °C. Consequently, it is found that oxygen diffuses within the PrO_δ planes and starts overcoming the surface energy barrier at unexpectedly low temperatures. Very likely, this temperature is determined by the surface exchange barrier (kinetics of oxygen exchange at the surface of the grains) rather than by the bulk oxygen diffusion.

The temperature dependences of the equilibrium oxygen content for different oxygen partial pressures were established for $PrBaCo_2O_{5+\delta}$ in the interval 5×10^{-4} to 180 atm. With the aid of these TGA measurements, after a careful choice of the annealing temperatures and times, we have been able to prepare four different samples having the desired stoichiometry. In particular, we prepared polycrystalline samples with the desired fractional values $\delta = {}^1/_2$ and ${}^3/_4$. The other two corresponded to stoichiometries near the extremes of low and high oxygenation (0.176 and 0.869). Although a large variation of the oxygen content was achieved in the Pr-layered "112" crystal structure, highly oxygenated samples can only be obtained using relatively high partial oxygen pressures. Using $P_{O_2} = 180$ atm, we obtained a maximum oxygen content of $\delta = 0.87(1)$, annealing the material at 190 °C. By means of NPD data, we have characterized these samples and, especially, the order arrangement of oxygen vacancies. This study contributes to establishing systematic ways to conveniently tailor the oxygen content in these interesting oxides.

Acknowledgment. Financial support by the Spanish MEC (MAT2003-07483-C02-02) and Generalitat de Catalunya (2001SGR-00334, PICS2005-14) projects is appreciated. C.F. acknowledges financial support from MEC (Spain). We acknowledge ILL and MEC (through ILL collaborating research group D1B CRG) for the provision of neutron-beam time. We also thank Dr. C. Ritter and Dr. E. Suard for their help during NPD data collection.

CM051148Q